Environmental Science & Technology Letters

Letter

pubs.acs.org/journal/estlcu

Determination of Iodide via Direct Fluorescence Quenching at Nitrogen-Doped Carbon Quantum Dot Fluorophores

Haimin Zhang,[†] Yibing Li,[†] Xiaolu Liu,[†] Porun Liu,[†] Yun Wang,[†] Taicheng An,*[,§] Huagui Yang,[†,∥] Dengwei Jing,[⊥] and Huijun Zhao*[,†,‡]

[†]Centre for Clean Environment and Energy, Griffith University, Gold Coast Campus, QLD 4222, Australia

[‡]Centre for Environmental and Energy Nanomaterials, Institutes of Solid State Physics, Chinese Academy of Sciences, Hefei 230031, China

[§]State Key Laboratory of Organic Geochemistry, Guangzhou Institute of Geochemistry, Chinese Academy of Sciences, Guangzhou 510640, China

[∥]Key Laboratory for Ultrafine Materials of Ministry of Education, School of Materials Science and Engineering, East China University of Science and Technology, 130 Meilong Road, Shanghai 200237, China

[⊥]State Key Laboratory of Multiphase Flow in Power Engineering, Xi'an Jiaotong University, 28 West Xianning Road, Xi'an City, Shanxi 710049, China

Supporting Information

ABSTRACT: The development of analytical methods for rapidly, sensitively, and selectively detecting iodide (I^-) in aqueous media is critically important because I^- is closely related to human health because of a number of diseases caused by the deficiency and radioactivity of I^-. In this work, we describe N-doped carbon quantum dots as the fluorophores for the direct determination of I^- fluorescence, achieving a detection limit of 10 μM with an analytical linear range up to 2.0 mM. The experimental results also demonstrate that the N-doped carbon quantum dot fluorophores possess high selectivity for I^- detection. The presence of nitrogen functional groups results in a positively charged carbon quantum dot surface, which is advantageous for the detection of I^- fluorescence because of the strong electrostatic interaction between carbon quantum dots and I^-. This work demonstrates the possibility of developing carbon quantum dot fluorophore-based fluorescence methods for the determination of other anions.

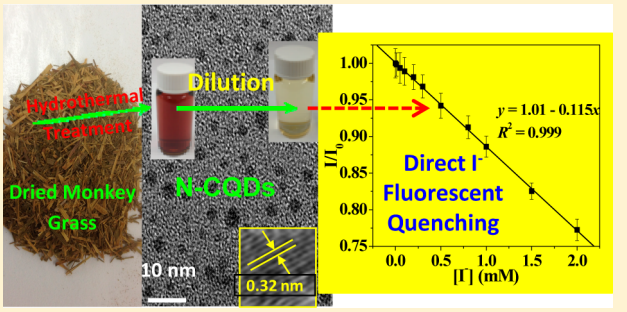

INTRODUCTION

Iodide (I^-) is widely distributed in aquatic environments and important for human health because a number of diseases are closely related to the deficiency and radioactivity of iodide.[1−5] Therefore, simple and rapid determination of I^- in an aquatic environment and radioactive wastes is important. Varieties of methods can be used to determine I^-, including fluorescence spectroscopy,[6,7] chromatography,[8] chemiluminescence,[9] chemosensing,[10] and electrochemical methods.[10,11] Among these methods, the fluorescence spectroscopic methods are widely used because of their rapidity, sensitivity, and selectivity.[12−14] Nevertheless, the fluorophores used by these methods are generally expensive, require complex preparation, and exhibit low hydrophilicity and poor dispersibility in water.[10,12] Therefore, the development of cheap fluorophores capable of sensitively and selectively determining iodide ion is needed.

Recently, a new class of carbon-based fluorophores [e.g., carbon quantum dots (CQDs) and nanodots (CNDs)] have been successfully synthesized.[15−19] The attractions of such forms of fluorophores lie in their superior fluorescence properties, cheap to produce and easy to handle, promising for fluorescence-based analytical applications.[15−19] To date, almost all reported CQD or CND fluorophores have been applied exclusively for the detection of cations, especially heavy metal ions, e.g., Cu^{2+} and Hg^{2+}.[7,17−20] To the best of our knowledge, CQD and CND fluorophores have not been applied in the direct detection of anions. Only CQD-based detection of the fluorescence of anions can be found in the recently published literature reported by Barman and coworkers for indirect I^- detection.[7] They smartly introduce I^- into a system containing the blue fluorescent CQDs quenched by Hg^{2+} (the quenching is highly sensitive and selective).[7] The quenching effect of Hg^{2+} is diminished because of the formation of the insoluble HgI_2 (K_{sp} = 2.8 × 10^{-29}), resulting a fluorescence intensity increase that is proportional to the I^-

Received: September 2, 2013
Revised: November 13, 2013
Accepted: November 14, 2013
Published: November 14, 2013

concentration.[7] A recent report indicated that the fluorescence of CNDs could be efficiently quenched by both the electron acceptor and the electron donor.[21] This suggests the possibility of utilizing directly anion quenching at the carbon-based fluorophores for the detection of the fluorescence of anions.

Herein, low-cost nitrogen-doped CQD (N-CQD) fluorophores with superior water dispersibility and fluorescence properties were successfully synthesized by hydrothermal treatment of dried monkey grass. We demonstrated for the first time that the fluorescence intensity of the N-CQD fluorophores can be directly quenched by iodide (I^-) in a highly selective and sensitive manner, which can be utilized to directly detect low concentrations of I^- in aqueous media.

MATERIALS AND METHODS

Synthesis of N-CQDs. N-CQDs were fabricated by a facile and one-pot hydrothermal method using dried monkey grass as a reaction precursor, as in a similar method reported previously (Figure 1A).[18] In a typical synthesis, 5.0 g of dried grass was added to 60 mL of deionized water (Milli-Q water, 18 MΩ), and then the mixture was transferred into a 100 mL Teflon-lined autoclave and kept at 180 °C for 6 h. After hydrothermal reaction, the N-CQD solution was collected by filtration (0.2 μm cellulose membrane) and centrifugation at 4500 and 12000 rpm for 10 min. The concentration of the as-synthesized N-CQDs is ~19 mg/mL. Using this method, the mass yield of N-CQDs can reach 22.8%. For the purpose of I^- detection, the as-synthesized N-CQD solution was further diluted 100-fold to obtain a dilute carbon quantum dot solution (Figure 1A). All N-CQD solutions were preserved for further characterization and use. For comparison, CQDs without nitrogen doping were also synthesized using a similar method reported by Li et al. for I^- detection.[22]

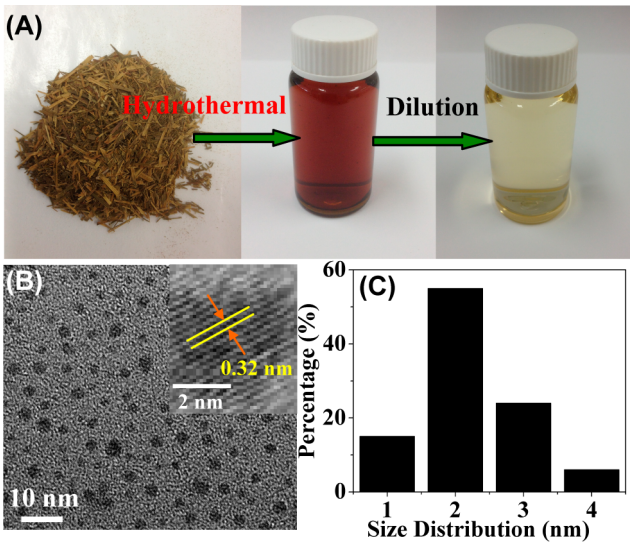

Figure 1. (A) Preparation of a N-doped carbon quantum dot (N-CQD) solution. (B) Transmission electron microscopy (TEM) image (inset, high-resolution TEM image) and (C) size distribution of N-CQDs.

Detection of Iodide (I^-). The detection of I^- was conducted at room temperature in a 0.2 M PBS (pH 7.0) buffer solution. In a typical experiment, 0.5 mL of an as-synthesized N-CQD solution at a concentration of 19 mg/mL was diluted to a total volume of 50 mL with a 0.2 M PBS buffer solution containing I^- at different concentrations. The photoluminescent (PL) spectra of the resulting samples were recorded after the sample had been held for 1.0 h at room temperature.

Characterizations. Transmission electron microscopy (TEM) analysis was performed using a Philips F20 electron microscope. The chemical composition of the N-CQD sample was analyzed using X-ray photoelectron spectroscopy (XPS) (Kratos Axis ULTRA instrument with a 165 mm hemispherical electron energy analyzer). All binding energies were carefully aligned by reference to the C1s peak (284.6 eV) arising from surface hydrocarbons or possible adventitious hydrocarbon. Fourier transform infrared (FT-IR) spectra of the N-CQD sample were analyzed by a Perkin-Elmer spectrum 1000 FT-IR spectrophotometer using KBr pellets. PL spectra of the N-CQD solutions without and with I^- were recorded with an F7000 fluorescence spectrophotometer (Hitachi) with excitation and emission slit widths of 0.5 mm. The excitation wavelength was set at 360 nm.

RESULTS AND DISCUSSION

A facile hydrothermal treatment of 5.0 g of dried monkey grass in 60 mL of Milli-Q water results in a brown-colored solution containing 19 mg/mL solid carbon materials, and the color becomes light yellow after 100-fold dilution (see Figure 1A). The solid carbon materials have been identified as N-doped CQDs.[18] A typical TEM image of the sample indicates that the sizes of the synthesized N-CQDs ranged from 1 to 4 nm, with ~55% being ~2 nm (Figure 1B,C). The high-resolution TEM image of the N-CQD displays a lattice spacing of ~0.32 nm (inset of Figure 1B), which is consistent with the ⟨002⟩ spacing of graphitic carbon.[23,24] This is also supported by X-ray diffraction (XRD) and UV−vis absorption results of the N-CQDs samples (Figure S1A,B of the Supporting Information).[25−27]

Further, FT-IR and XPS analyses confirm that the synthesized CQDs possess rich surface O- and N-function groups such as C−O, C═O, O−H, C−N, C═N, C−N−C, $N-(C)_3$, and N−H (Figure 2), results similar to those previously reported.[18,27] The presence of N-function groups can lead to a positively charged CQD surface,[18] which might be beneficial for the detection of the fluorescence of anions because of the strong electrostatic interaction with anions.[28,29] The ζ potential measurement of N-CQDs indicates a positive surface potential of 30.2 mV, further confirming that N-doping can introduce positive charges into the surrounding graphitic carbon network.[18] The XPS surface survey spectra (Figure 2B) show that the synthesized N-CQDs contain high oxygen content because of the formation of O-rich function groups during hydrothermal reaction (see the high-resolution XPS spectrum of oxygenin Figure S2 of the Supporting Information).[18,27] In this work, the dilute solution containing 0.19 mg/mL dispersed N-CQD fluorophores is used for subsequent I^- detection.

The fluorescence of the N-CQD fluorophores was first investigated. Figure 3A shows the PL excitation and emission spectra of the N-CQD solution. As shown, the N-CQD fluorophores can be excited by wavelengths between 340 and 370 nm (black curve). When the excitation wavelength is set at 360 nm, a strong PL emission peak centered at ~435 nm can clearly be observed (red curve). The photograph (inset of Figure 3A) of the N-CQD fluorophore solution under 365 nm UV irradiation displays a bright blue color, confirming the

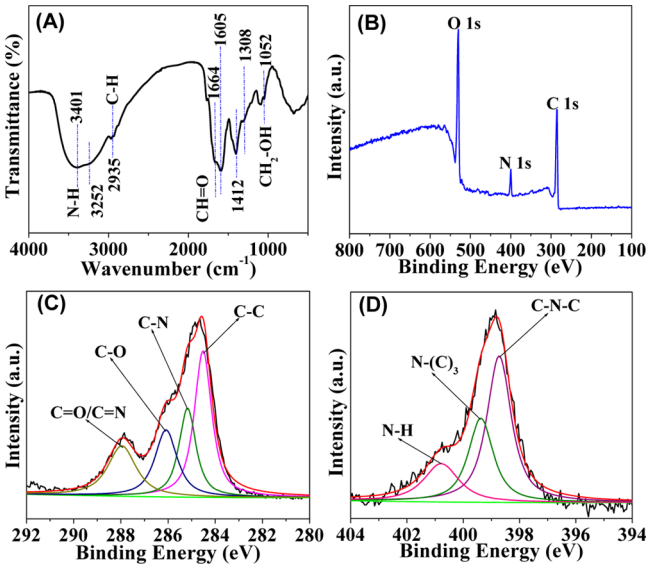

Figure 2. (A) FT-IR spectra, (B) XPS survey spectra, (C) C1s high-resolution XPS spectra, and (D) N1s high-resolution XPS spectra of N-CQDs.

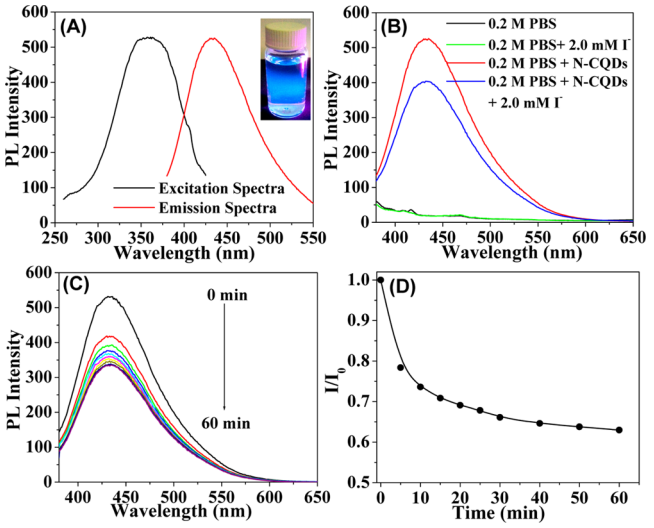

Figure 3. (A) PL excitation and emission spectra of the N-CQDs. (B) PL emission spectra of 0.2 M PBS, 0.2 M PBS with 2.0 mM I^-, 0.2 M PBS with N-CQDs, and 0.2 M PBS with N-CQDs and 2.0 mM I^-. (C) Time-dependent PL spectra of N-CQDs quenched with 5.0 mM I^-. (D) Time-dependent relative PL peak intensities derived from panel C. The excitation wavelength was 360 nm.

strong blue fluorescence of the N-CQD fluorophore, which is favorable for fluorescence-based analytical applications.[7,18] In this work, the PBS buffer solution (0.2 M, pH 7.0) was used to achieve better reproducibility and accuracy. As shown in Figure 3B, the PBS buffer detection medium does not contribute to PL emission for I^- quenching. The PL intensity of the N-CQD solution noticeably decreased when 2.0 mM I^- was introduced, resulting from the direct I^- quenching. Such an observed quenching phenomenon provides a solid basis for analytical determination of I^- in aqueous media. Figure 3C shows the time-dependent PL spectra of the N-CQD solution quenched with 5.0 mM I^- excited at 360 nm. As shown, the introduction of I^- leads to a rapid decrease in the PL intensity during the initial 10 min. The PL intensity gradually levels off at relatively stable values with a further increased quenching time (Figure 3D). For better accuracy and reproducibility, all PL intensities are measured after reactions had been quenched for 1 h for subsequent experiments.

The analytical performance of the N-CQD fluorophores was evaluated for determination of I^-. As expected, the PL intensity excited at 360 nm decreases with an increasing I^- concentration (Figure 4A). The inset of Figure 4A shows the relationship

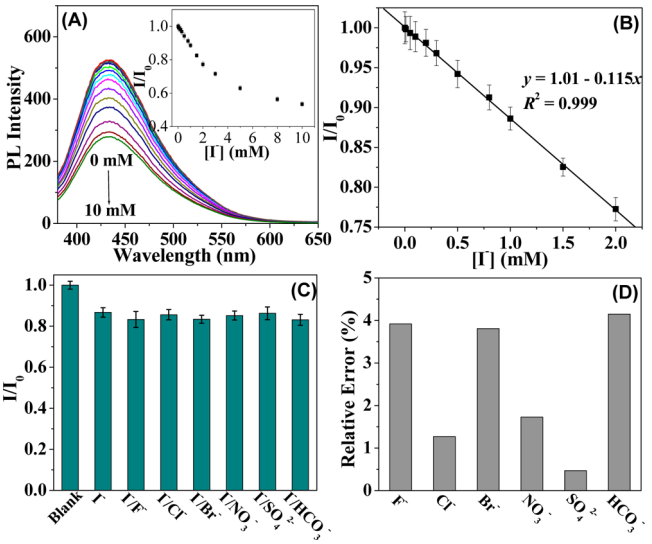

Figure 4. (A) PL spectra of N-CQDs with different I^- concentrations (inset, dependence of the relative PL peak intensity on I^- concentration within the range of 0–10 mM). (B) Plot of the relative PL peak intensity vs I^- concentration from 0 to 2.0 mM. (C) Interference of common anions with relative PL peak intensities at 1.0 mM I^- and 100 mM interference anion. The PL peak intensity of the blank equals I_0. (D) Relative error caused by different interference anions.

between the relative PL peak intensity and I^- concentration, derived from the PL spectra in Figure 4A. It can be seen that the relative PL peak intensity decreases linearly at low I^- concentrations and deviates from the linear response when the I^- concentration is higher. An excellent linear relationship (R^2 = 0.999) was observed within the concentration range of 0–2.0 mM (Figure 4B). This demonstrates that the relative PL peak intensity change of the N-CQD fluorophores that resulted from the direct I^- quenching can be used as the analytical signal for I^- detection. Under such conditions, a detection limit of 10 μM can be achieved, comparable to the reported fluorescence method using other fluorophores.[12] Compared to other detection methods such as the electrochemical approach (detection limit of 0.5 μM),[11] the gold nanoparticle-based fluorescence method (detection limit of 50 nM),[30] and the indirect fluorescence detection approach (detection limit of ~10^{-9} M),[7] although the detection limit of I^- in this work is higher, the proposed method has advantages over other methods, including its simplicity in analytical operation and inexpensive nature of N-CQD fluorophores. Also, from a scientific point of view, the demonstrated direct I^- fluorescence quenching analytical principle paves the way for applications of N-CQD fluorophores for direct fluorescence detection of other anions.

The selectivity is critically important in determining the applicability of an analytical method. Figure 4C shows the

interference of the common anions with the relative PL peak intensity. All experiments were conducted under competitive quenching conditions with an I^- to interference anion concentration ratio of 1/100 (1.0 mM I^- and 100 mM interference anion). As shown in Figure 4D, the relative errors caused by all interference anions investigated are below ~5.0%, demonstrating a high selectivity of N-CQD fluorophores for I^- detection. Although good selectivity of N-CQD fluorophores toward I^- detection has been experimentally demonstrated, the precise reason(s) is unclear. However, the positively charged N-CQD surface (as confirmed by the measured ζ potential) could be an important attribute as it allows strong electrostatic interactions with I^-. To confirm the importance of N-doping, the experiments using CQDs without nitrogen doping as the fluorophores for I^- detection were performed. The results indicate that the CQDs without nitrogen doping exhibit very poor sensitivity for I^- detection (see Figure S3 of the Supporting Information) because of the negatively charged CQD surface.[15] It is a common knowledge that I^- is one of the largest monatomic anions, making it a typical soft Lewis base that can readily change its spatial shape during interaction with hard Lewis acids. Such an inherent property of I^- makes it more favorable than harder Lewis anion bases (e.g., F^-, Cl^-, SO_4^{2-}, HCO_3^-, CO_3^{2-}, and NO_3^-) in matching the spatial configuration of self-trapped excitons at N-CQDs that allows strong interactions with N-CQDs, giving rise to good selectivity.[31]

Further, the tap water and lake water were used to test the applicability of the N-CQD fluorophore method for real sample analysis. The sampled tap water and lake water mainly contain anions such as F^-, Cl^-, SO_4^{2-}, HCO_3^-, CO_3^{2-}, and NO_3^-. In this work, the concentration of I^- in these samples was found to be below the detection limit. The recovery experiments were therefore performed using tap water and lake water samples as a matrix to validate the method. Table 1 shows the experimental recovery results. It can be seen that upon addition of 50, 200, and 600 μM I^-, the percentage recoveries are between 98 and 105% for the tap water matrix and 97 and 108% for the lake water matrix. Such excellent recovery results suggest that the N-CQD fluorophore method can be used for the detection of I^- in freshwater samples.

Table 1. Recovery of I^- from Real Water Samples

sample	added I^- (μM)	measured I^- (μM)	recovery (%)	relative standard deviation (%) (n = 3)
tap water	50	51.2	102	2.7
	200	196	98	2.1
	600	631	105	1.6
lake water	50	48.5	97	2.3
	200	207	104	2.6
	600	648	108	1.8

In summary, we have demonstrated for the first time the use of N-CQDs as effective fluorophores for selective determination of I^- via a direct fluorescence quenching principle. The attractions of such N-CQD fluorophores are their inexpensive nature, their ease of acquisition, and their ease of use. Our findings pave the way for developing N-CQD fluorophore-based fluorescence methods for the determination of other anions.

■ ASSOCIATED CONTENT

Supporting Information

XRD patterns and UV−vis absorption spectra of N-CQDs (Figure S1), O1s high-resolution XPS spectra of N-CQDs (Figure S2), and PL emission spectra of 0.2 M PBS with CQDs without nitrogen doping and 0.2 M PBS with CQDs without nitrogen doping with 10 mM I^- (Figure S3). This material is available free of charge via the Internet at http://pubs.acs.org.

■ AUTHOR INFORMATION

Corresponding Authors

*Telephone: +61 7 55528261. Fax: +61 7 55528067. E-mail: h.zhao@griffith.edu.au.

*E-mail: antc99@gig.ac.cn.

Notes

The authors declare no competing financial interest.

■ ACKNOWLEDGMENTS

This work was financially supported by the Australian Research Council Discovery Project.

■ REFERENCES

(1) Gerard, A.-C.; Humblet, K.; Wilvers, C.; Poncin, S.; Derradji, H.; de Ville de Goyet, C.; Abou-el-Ardat, K.; Baatout, S.; Sonveaux, P.; Denef, J.-F.; Colin, I. M. Iodine-deficiency-induced long lasting angiogenic reaction in thyroid cancers occurs via a vascular endothelial growth factor-hypoxia inducible factor-1-dependent, but not a reactive oxygen species-dependent, pathway. *Thyroid* **2012**, *22*, 699−708.

(2) Meletis, C. D. Iodine: Health implications of deficiency. *J. Evidence-Based Complementary Altern. Med.* **2011**, *16*, 190−194.

(3) Daraoui, A.; Michel, R.; Gorny, M.; Jakob, D.; Sachse, R.; Synal, H. A.; Alfimov, V. Iodine-129, iodine-127 and caesium-137 in the environment: Soils from Germany and Chile. *J. Environ. Radioact.* **2012**, *112*, 8−22.

(4) Haymart, M. R.; Muenz, D. G.; Stewart, A. K.; Griggs, J. J.; Banerjee, M. Disease severity and radioactive iodine use for thyroid cancer. *J. Clin. Endocrinol. Metab.* **2013**, *98*, 678−686.

(5) Jhummon, N. P.; Tohooloo, B.; Qu, S. Iodine-131 induced hepatotoxicity in previously healthy patients with Grave's disease. *Thyroid Res.* **2013**, *6*, 4.

(6) Zhang, M.; Ye, B.-C. A reversible fluorescent DNA logic gate based on graphene oxide and its application for iodide sensing. *Chem. Commun.* **2012**, *48*, 3647−3649.

(7) Barman, S.; Sadhukhan, M. Facile bulk production of highly blue fluorescent graphitic carbon nitride quantum dots and their application as highly selective and sensitive sensors for the detection of mercuric and iodide ions in aqueous media. *J. Mater. Chem.* **2012**, *22*, 21832−21837.

(8) Mura, P.; Papet, Y.; Sanchez, A.; Piriou, A. Rapid and specific high-performance liquid chromatographic method for the determination of iodide in urine. *J. Chromatogr., B* **1995**, *664*, 440−443.

(9) Fujiwara, T.; Inoue, H.; Mohammadzai, I. U.; Kumamaru, T. Chemiluminescence determination of iodide and/or iodine using a luminol-hexadecyltrimethylammonium chloride reversed micelle system following on-line oxidation and extraction. *Analyst* **2000**, *125*, 759−763.

(10) Wang, G.-L.; Zhu, X.-Y.; Dong, Y.-M.; Jiao, H.-J.; Wu, X.-M.; Li, Z.-J. The pH-dependent interaction of silver nanoparticles and hydrogen peroxide: A new platform for visual detection of iodide with ultra-sensitivity. *Talanta* **2013**, *107*, 146−153.

(11) Ibupoto, Z. H.; Khun, K.; Willander, M. A selective iodide ion sensor electrode based on functionalized ZnO nanotubes. *Sensors* **2013**, *13*, 1984−1997.

(12) Geddes, C. D. Optical halide sensing using fluorescence quenching: Theory, simulations and applications—a review. *Meas. Sci. Technol.* **2001**, *12*, R53−R88.

(13) Kramer, R. Fluorescent chemosensors for Cu^{2+} ions: Fast, selective, and highly sensitive. *Angew. Chem., Int. Ed.* **1998**, *37*, 772−773.
(14) Xu, L.; Zhang, D.; Huang, J.; Deng, M.; Zhang, M.; Zhou, X. High fluorescence selectivity and visual detection of G-quadruplex structures by a novel dinuclear ruthenium complex. *Chem. Commun.* **2010**, *46*, 743−745.
(15) Li, H.; Kang, Z.; Liu, Y.; Lee, S.-T. Carbon nanodots: Synthesis, properties and applications. *J. Mater. Chem.* **2012**, *47*, 24230−24253.
(16) Baker, S. N.; Baker, G. A. Luminescent carbon nanodots: Emergent nanolights. *Angew. Chem., Int. Ed.* **2010**, *49*, 6726−6744.
(17) Zhou, L.; Lin, Y.; Huang, Z.; Ren, J.; Qu, X. Carbon nanodots as fluorescence probes for rapid, sensitive, and label-free detection of Hg^{2+} and biothiols in complex matrices. *Chem. Commun.* **2012**, *48*, 1147−1149.
(18) Liu, S.; Tian, J.; Wang, L.; Zhang, Y.; Qin, X.; Luo, Y.; Asiri, A. M.; Al-Youbi, A. O.; Sun, X. Hydrothermal treatment of grass: A low-cost, green route to nitrogen-doped, carbon-rich, photoluminescent polymer nanodots as an effective fluorescent sensing platform for label-free detection of Cu(II) ions. *Adv. Mater.* **2012**, *24*, 2037−2041.
(19) Dong, Y.; Wang, R.; Li, G.; Chen, C.; Chi, Y.; Chen, G. Polyamine-functionalized carbon quantum dots as fluorescent probes for selective and sensitive detection of copper ions. *Anal. Chem.* **2012**, *84*, 6220−6224.
(20) Qu, Q.; Zhu, A.; Shao, X.; Shi, G.; Tian, Y. Development of a carbon quantum dots-based fluorescent Cu^{2+} probe suitable for living cell imaging. *Chem. Commun.* **2012**, *48*, 5473−5475.
(21) Wang, X.; Cao, L.; Lu, F.; Meziani, M. J.; Li, H.; Qi, G.; Zhou, B.; Harruff, B. A.; Kermarrec, F.; Sun, Y.-P. Photoinduced electron transfers with carbon dots. *Chem. Commun.* **2009**, 3774−3776.
(22) Li, H.; He, X.; Liu, Y.; Huang, H.; Lian, S.; Lee, S.-T.; Kang, Z. One-step ultrasonic synthesis of water-soluble carbon nanoparticles with excellent photoluminescent properties. *Carbon* **2011**, *49*, 605−609.
(23) Wang, C.; Wu, X.; Li, X.; Wang, W.; Wang, L.; Gu, M.; Li, Q. Upconversion fluorescent carbon nanodots enriched with nitrogen for light harvesting. *J. Mater. Chem.* **2012**, *22*, 15522−15525.
(24) Li, H.; He, X.; Kang, Z.; Huang, H.; Liu, Y.; Liu, J.; Lian, S.; Tsang Chi Him, A.; Yang, X.; Lee, S.-T. Water-soluble fluorescent carbon quantum dots and photocatalyst design. *Angew. Chem., Int. Ed.* **2010**, *49*, 4430−4434.
(25) Bethune, D.; Kiang, C.; Devries, M.; Gorman, G.; Savoy, R.; Beyers, R. The discovery of single-wall carbon nanotubes at IBM. *Nature* **1993**, *363*, 605−607.
(26) Kang, Z.; Wang, E.; Gao, L.; Lian, S.; Jiang, M.; Hu, C.; Xu, L. One-step water-assisted synthesis of high-quality carbon nanotubes directly from graphite. *J. Am. Chem. Soc.* **2003**, *125*, 13652−13653.
(27) Li, Y.; Zhao, Y.; Cheng, H.; Hu, Y.; Shi, G.; Dai, L.; Qu, L. Nitrogen-doped graphene quantum dots with oxygen-rich functional groups. *J. Am. Chem. Soc.* **2012**, *134*, 15−18.
(28) Choi, K.; Hamilton, A. D. A dual channel fluorescence chemosensor for anions involving intermolecular excited state proton transfer. *Angew. Chem., Int. Ed.* **2001**, *40*, 3912−3915.
(29) Kuo, L.-J.; Liao, J.-H.; Chen, C.-T.; Huang, C.-H.; Chen, C.-S.; Fang, J.-M. Two-arm ferrocene amide compounds: Synclinal conformations for selective sensing of dihydrogen phosphate ion. *Org. Lett.* **2003**, *5*, 1821−1824.
(30) Chen, Y.-M.; Cheng, T.-L.; Tseng, W.-L. Fluorescence turn-on detection of iodide, iodate and total iodine using fluorescein-5-isothiocyanate-modified gold nanoparticles. *Analyst* **2009**, *134*, 2106−2112.
(31) Li, A.-F.; Wang, J.-H.; Wang, F.; Jiang, Y.-B. Anion complexation and sensing using modified urea and thiourea-based receptors. *Chem. Soc. Rev.* **2010**, *39*, 3729−3745.